Bioorganic & Medicinal Chemistry Letters 19 (2009) 6386–6391

Contents lists available at ScienceDirect

Bioorganic & Medicinal Chemistry Letters

journal homepage: www.elsevier.com/locate/bmcl

Design and synthesis of cell potent BACE-1 inhibitors: Structure–activity relationship of *P*1′ substituents

Jennifer M. Sealy [a], Anh P. Truong [a], Luke Tso [a], Gary D. Probst [a,*], Jose Aquino [a], Roy K. Hom [a,*], Barbara M. Jagodzinska [a], Darren Dressen [a], David W. G. Wone [a], Louis Brogley [a], Varghese John [a], Jay S. Tung [a], Michael A. Pleiss [a], John A. Tucker [a], Andrei W. Konradi [a], Michael S. Dappen [b], Gergely Toth [c], Hu Pan [c], Lany Ruslim [d], Jim Miller [d], Michael P. Bova [d], Sukanto Sinha [d], Kevin P. Quinn [e], John-Michael Sauer [e]

[a] *Department of Medicinal Chemistry, Elan Pharmaceuticals, 180 Oyster Point Boulevard, South San Francisco, CA 94080, United States*
[b] *Department of Process and Analytical Chemistry, Elan Pharmaceuticals, 180 Oyster Point Boulevard, South San Francisco, CA 94080, United States*
[c] *Department of Molecular Design, Elan Pharmaceuticals, 180 Oyster Point Boulevard, South San Francisco, CA 94080, United States*
[d] *Department of Biology, Elan Pharmaceuticals, 1000 Gateway Boulevard, South San Francisco, CA 94080, United States*
[e] *Department of Lead Finding, Drug Disposition, and Safety Evaluation, Elan Pharmaceuticals, 800 Gateway Boulevard, South San Francisco, CA 94080, United States*

ARTICLE INFO

Article history:
Received 8 August 2009
Revised 14 September 2009
Accepted 16 September 2009
Available online 19 September 2009

Keywords:
Alzheimer's disease
β-Secretase (BACE-1) inhibitor
Hydroxyethylamine (HEA)

ABSTRACT

Using structure-guided design, hydroxyethylamine BACE-1 inhibitors were optimized to nanomolar Aβ cellular inhibition with selectivity against cathepsin-D. X-ray crystallography illuminated the *S*1′ residues critical to this effort, which culminated in compounds **56** and **57** that exhibited potency and selectivity but poor permeability and high P-gp efflux.

Alzheimer's disease (AD) is a form of senile dementia, characterized by a progressive loss of memory and cognitive ability, affecting 24 million elderly people worldwide.[1] The pathology of this neurodegenerative disorder uniquely manifests itself with the presence of extraneuronal aggregation of plaques composed of β-amyloid peptides (Aβ).[2] Aβ-peptides are derived from the sequential proteolytic cleavage of the β-amyloid precursor protein (β-APP) by two aspartic acid proteases, referred to as β- and γ-secretase, respectively.[3] Inhibition of either protease has been demonstrated to result in reduction of brain Aβ-peptide in preclinical studies.[4] Inhibitors of either protease offer attractive candidates as disease-modifying treatments for people afflicted with this debilitating malady.[5]

Between these two proteases, β-secretase (BACE-1) is the more alluring therapeutic target based on the following distinctions. γ-Secretase processes a myriad of substrates,[6] such as Notch, raising concerns about mechanism-based side-effects due to a deficiency in selectivity.[7] Conversely, gene deletion of BACE-1 in mice produced no consistent phenotypic differences between their *wild type* counterparts.[8] These knockout mice are without compensatory activity, thus devoid of the ability to generate Aβ in the brain.[9] Furthermore, modest reductions of BACE-1 activity have resulted in significant reductions in plaque burden.[10] Additionally, cleavage of β-APP by BACE-1 is the rate-limiting step in Aβ-peptide production[3] and releases the soluble N-terminal APP fragment (sAPP-β) which triggers a cascade event ultimately leading to neurodegeneration.[11] This validates BACE-1 and presents its clear advantages over γ-secretase as a therapeutic target.

Our goal was to develop cell potent BACE-1 inhibitors that were selective over closely related aspartyl proteases such as cathepsin-D (cat-D) due to potential toxicity.[12] To effect this, we implemented a strategy to exploit the sequence differences between BACE-1 and cat-D in the *S*1′ pocket.[13] Herein, we describe a general binding mode of hydroxyethylamines (HEA) to BACE-1, and specifically the amino acid residues that comprise the *S*1′ pocket. From these differences arose the strategy toward selectivity while enhancing cell potency.

The X-ray crystal structure of BACE-1 and compound **1**[14] illustrates the active site binding mode (Figs. 1 and 2). The difluoroaryl, cyclohexyl, and *tert*-butyl substituents occupy the *S*1, *S*1′, and *S*2′ pockets, respectively, as shown in Figures 1 and 2. The *S*1′ pocket

* Corresponding authors. Tel.: +1 650616 2684; fax: +1 650794 2387 (G.D.P.), tel.: +1 650616 5061; fax: +1 650794 2458 (R.K.H.).
E-mail addresses: gary.probst@elan.com (G.D. Probst), roy.hom@elan.com (R.K. Hom).

0960-894X/$ - see front matter © 2009 Elsevier Ltd. All rights reserved.
doi:10.1016/j.bmcl.2009.09.061

Table 1
SAR of the P1′ ring sizes and oxygen containing heterocycles

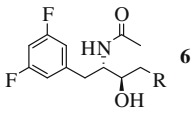

6

#	R	BACE IC_{50}[a] (nM)	Cat D IC_{50}[b] (nM)	Cell ED_{50}[c] (nM)
1	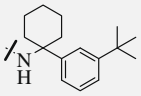	47	25	17
7	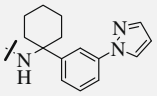	59	22	4.0
8	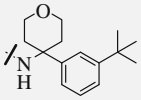	61	230	15
9[d]	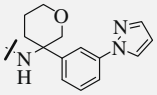	270	170	91
10	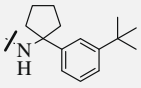	220	130	>100
11[d]	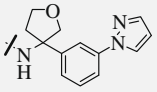	2400	4900	>1000

[a] See Ref. 17.
[b] See Ref. 18.
[c] See Ref. 19.
[d] 1:1 mixture of epimers.

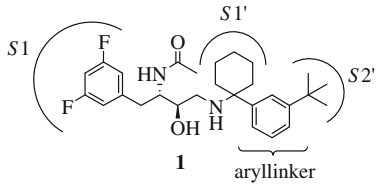

Figure 1. Binding mode of the HEAs to BACE-1.

is amphiphilic in nature. The 'backside' is bordered by two hydrophobic residues Val332 and Ile226. Two hydrophilic residues Lys227 and Thr329 constitute the 'top', and the 'right side' consists of Tyr198 and Gly34 (Fig. 3). The 'left side' contains Arg235 and Thr72 which is part of the flap, while Asp228 and Thr231 compose the 'bottom' (Fig. 4). The protonated amino and hydroxyl group binds at the scissle site to Asp32 and Asp228, respectively (not shown). The carbonyl of Gly34 also forms a hydrogen bond with the ionized amine and hydrogen on the aryl linker flanked by the two alkyl groups (not shown).[15] The acetamide functions as a bidentate ligand with the carbonyl forming a hydrogen bond with the flap residue Gln73 while the NH interacts with Gly230 (not shown).

An exemplary synthetic route employed to construct the HEA inhibitors is outlined in Scheme 1. An aryl lithium was generated

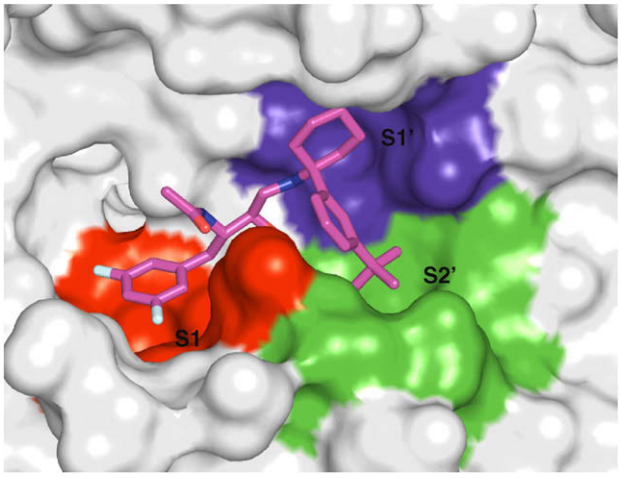

Figure 2. Crystal structure of **1** binding to truncated (56–455) human BACE-1 (1.8 Å resolution). The PBD deposition code is 3ivh.

from **3** and added to a variety of cyclic ketones to produce tertiary alcohols which were converted to azides followed by subsequent reduction to amine **4**. Alkylation of the epoxide **5**[16] by the amine **4**, deprotection, and acetylation of the primary amine afforded the desired compound **1**.

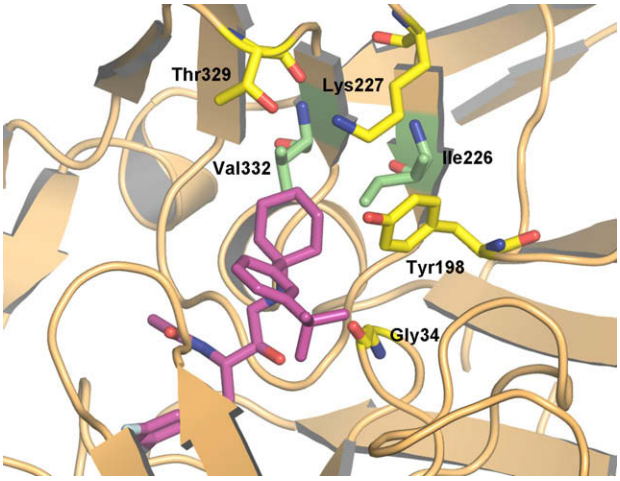

Figure 3. The *S1′* pocket: the 'backside', 'top', and 'right side' residues.

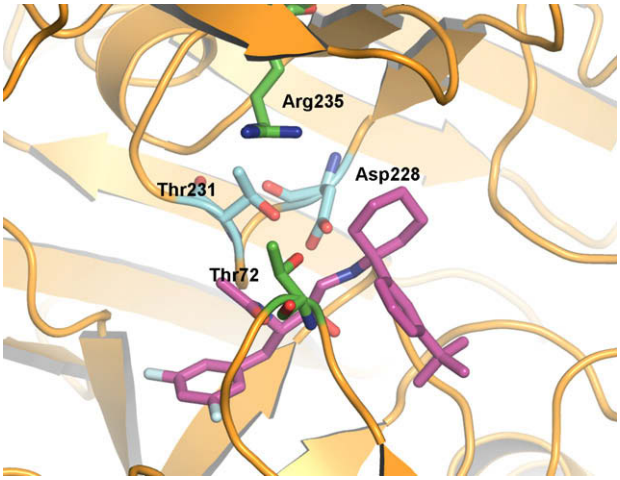

Figure 4. The *S1′* pocket: the 'left side' and 'bottom' residues.

During the course of our studies, we discovered that occupying space in the *S1′* pocket resulted in a significant increase in potency with six-membered rings being the most potent amongst the various ring sizes (e.g., **1** vs **10**) (see Table 1). To further increase potency and selectivity we sought to establish contact with the hydrophilic residues, Lys227 and/or Thr329, at the 'top' of the *S1′* pocket by placing an oxygen atom in the ring at the position distal to the amine. The pyran **8** did not enhance potency relative to **1** but it did reverse the selectivity bestowing a modest fourfold increase in selectivity for BACE-1 over cat-D. Molecular modeling suggested that compounds **9** and **11** could make contact with the phenol of Tyr198, but both modifications failed to increase potency.

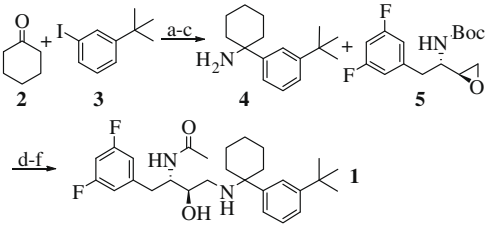

Scheme 1. Reagents and conditions: (a) *n*-BuLi, THF, −78 °C, 65%; (b) $TMSN_3$, BF_3–OEt_2, CH_2Cl_2, reflux or TFA, NaN_3, CH_2Cl_2, reflux, 45%; (c) $LiAlH_4$, Et_2O, 0 °C or 10% Pd/C, H_2, EtOAc, 100%; (d) *N,N*-diisopropylethylamine, isopropanol, reflux, 60%; (e) 4 N HCl in dioxane; (f) Ac_2NOMe, triethylamine, CH_2Cl_2, 90% over two steps.

We also examined the SAR of two series of nitrogen containing heterocycles (Tables 2 and 3). The results from both series of piperdines were disappointing except for the hydroxyl amine **19**, which displayed a similar cellular potency and a slight selectivity for BACE-1 over cat-D relative to **1**. The δ-lactams **15** and **16** were significantly more selective for BACE-1 over cat-D compared to **1** and slightly more potent against BACE-1 but with similar cellular activity.

The δ-lactam **23** in Table 3 was synthesized via the route outlined in Scheme 2. A palladium-catalyzed arylation[20] between **24** and **3**, followed by Michael addition with ethyl acrylate, and reduction of the nitrile afforded the δ-lactam. Installation of the amine

Table 2
SAR of nitrogen containing heterocycles at the 4-position

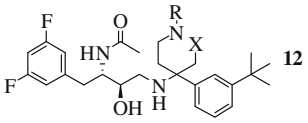

#	X	R	BACE IC_{50}[a] (nM)	Cat D IC_{50}[b] (nM)	Cell ED_{50}[c] (nM)
13	CH_2	H	4700	>10,000	710
14	CH_2	$CONH_2$	380	4300	>1000
15[d]	CO	H	18	330	21
16[d]	CO	H	19	1100	23

[a] See Ref. 17.
[b] See Ref. 18.
[c] See Ref. 19.
[d] Separated single diastereomer.

Table 3
SAR of nitrogen containing heterocycles at the 3-position

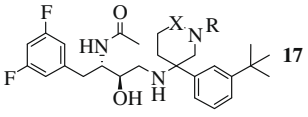

#[a]	X	R	BACE IC_{50}[b] (nM)	Cat D IC_{50}[c] (nM)	Cell ED_{50}[d] (nM)
18	CH_2	H	>10,000	2327	>1000
19	CH_2	OH	400	670	45
20	CH_2	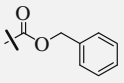	860	3.3	780
21	CH_2	COMe	1300	410	560
22	CH_2	$CONH_2$	330	90	210
23	CO	H	47	180	76

[a] All compounds are 1:1 mixture of epimers.
[b] See Ref. 17.
[c] See Ref. 18.
[d] See Ref. 19.

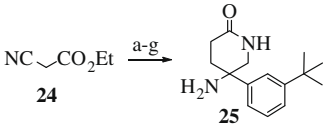

Scheme 2. Reagents and conditions: (a) **3**, $Pd_2(dba)_3$–$CHCl_3$, P(*tert*-Bu)$_3$–HBF_4, Na_3PO_4, PhMe, 100 °C, 57%; (b) ethyl acrylate, EtONa, EtOH, 71%; (c) Raney Ni, H_2, EtOH, then 75 °C, 69%; (d) NH_2NH_2–H_2O, EtOH; (e) $NaNO_2$, AcOH, H_2O; (f) 2-trimethylsilylethanol, PhMe, reflux, 66% over three steps; (g) TBAF, THF, reflux, 78%.

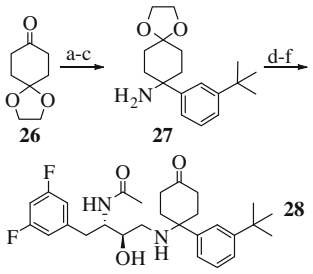

Scheme 3. Reagents and conditions: (a) *tert*-butylsulfinamide, $Ti(OEt)_4$, THF, 60%; (b) **3**, *n*-BuLi, THF, −78 °C, 47%; (c) HCl in Et_2O, 95%; (d) **5**, *N,N*-diisopropylethylamine, isopropanol, reflux, 62%; (e) 4 N HCl in dioxane; (f) Ac_2NOMe, triethylamine, CH_2Cl_2, 71% over two steps.

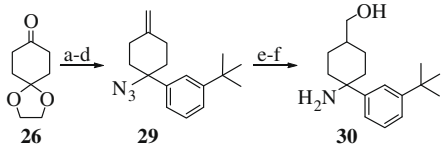

Scheme 4. Reagents and conditions: (a) *n*-BuLi, Ph_3PCH_3Br, THF, 0 °C, 79%; (b) 10% aq HCl, THF, 88%; (c) **3**, *n*-BuLi, THF, −78 °C, 81%; (d) $TMSN_3$, BF_3–OEt_2, CH_2Cl_2, reflux, 37%; (e) 9-BBN, THF, then aq NaOH, 30% H_2O_2, 0 °C, 3:1 trans:cis 79%; (f) 10% Pd/C, H_2, EtOAc, 100%.

via a Curtius rearrangement followed by deprotection afforded **25**. Standard chemistry (vide supra) completed the synthesis of **23**.

Next, our attention turned to the exploration of the substituents at the 4-position of the cyclohexyl ring. Condensation of the ketone **26** with *tert*-butylsulfinamide followed by addition of an aryl lithium, and subsequent removal of the sulfinyl group afforded intermediate **27** which in turn produced **28** via previously described chemistry (Scheme 3). This ketone proved to be a versatile intermediate to derivatize (e.g., reductive aminations). Compound **29** was constructed by standard chemistry previously discussed in this paper and served as a versatile intermediate that led to the synthesis of **34**, **36**, and **37** (Scheme 4 and Table 4).

Substituents trans to the amine were invariably more active than the corresponding cis isomer (e.g., **33** vs **32**, respectively) (Table 4). The trans alcohol **33** was twice as potent as **1**, had similar cellular activity, and displayed a selectivity of 58-fold over cat-D. In general, the BACE-1 SAR remained relatively flat with respect to lipophilic or hydrophilic substituents placed at the 4-position (**33**–**34** and **36**–**39**) until a breakthrough discovery with the ketoxime **43**. This functional group simultaneously donates and accepts hydrogen bonds which led to a fivefold increase in potency, nearly 2 orders of magnitude of improvement in selectivity over cat-D, and a 19-fold enhancement in cellular activity relative to **1**. This moiety was hydrolytically unstable, so the search for other donor/acceptors groups was initiated. Only the hydroxylamine **44**, which may not be a pharmaceutically acceptable functional group,[21] was comparable to **43** in the enzymatic and cellular assays, and exhibited greater than 200-fold selectivity for BACE-1 over cat-D. Several other donor/acceptor functionalities resulted in reduced potencies of 100–400 nM against BACE-1, but still exhibited excellent cellular activities of 1.3–16 nM (**45**–**49**). An *N*-aryl series (**51**–**52**) of inhibitors attained results comparable to **1** but were significantly more selective for BACE-1 over cat-D.

We hypothesized that an aromatic ring would be a chemically stable surrogate for the ketoxime **43**. The amine in intermediate **27** was protected as the carbamate, Bredereck's reagent was utilized to generate the vinylogous amide **54** which served as the key intermediate for the rapid synthesis of a diverse set of heterocycles such as the pyrazole **55** (Scheme 5).

Gratifyingly, the pyrazole **56** and 2-aminopyrimidine **57** was nearly as potent as **43** in both the biochemical and cellular assays,

Table 4
SAR of substituents distal to the amine

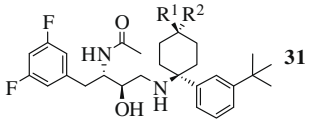

#	R^1	R^2	BACE IC_{50}[a] (nM)	Cat D IC_{50}[b] (nM)	Cell ED_{50}[c] (nM)
28	—	=O	120	450	5.6
32	OH	H	9200	>10,000	870
33	H	OH	24	1400	11
34	H	CH_2OH	38	330	31
35	H	CH_2CH_2OH	>10,000	>10,000	>1000
36	—	$=CH_2$	48	22	15
37	H	Me	49	80	17
38	H	SMe	24	84	7.5
39	H	CF_3	33	28	54
40	H	OMe	140	130	13
41	H	CN	380	640	37
42	H	SO_2Me	210	2300	100
43	—	=NOH	8.8	430	0.89
44	H	NHOH	19	3900	0.96
45	H	NHOMe	100	530	7.6
46	H	$NHCO_2Me$	240	2000	16
47	H	NHCHO	210	>10,000	2.4
48	H	$NHSO_2Me$	400	7200	5.9
49	H	N(OH)Ac	240	2300	1.3
50	H	NHAc	350	>10,000	48
51	H	NH-2-pyridine	73	4400	21
52	H	NH-2-thiazole	85	3100	18
53	H	NH-3-pyridine	500	9800	na

[a] See Ref. 17.
[b] See Ref. 18.
[c] See Ref. 19.

and exhibited selectivity over cat-D of 25- and 15-fold, respectively (Table 5). Furthermore, both **56** and **57** exhibited excellent cell ED_{50} of 2 nM. The co-crystal structure of the active diastereomer of **56** (Fig. 5) clearly shows the pyrazole functioning as a bi-dentate ligand hydrogen bonding to both Thr329 and Lys227 residues at a distance of 2.9 Å (see Fig. 5).

Unfortunately, the permeability for all of these compounds was poor except for the pyran **8**, which displayed moderate permeability (Table 6). More importantly from a drug properties perspective, all of these compounds showed an unacceptable Permeability-glycoprotein (P-gp) efflux liability. This combination of poor permeability and high efflux was not conducive to penetration into the brain parenchyma to exert the desired pharmacodynamic effect.

In conclusion, via structure-guided design we synthesized cell potent nanomolar BACE-1 inhibitors with good selectivity over cat-D. The cell-to-enzyme ratios were excellent possibly due to compartmentalization,[24] resulting in higher local concentrations relative to the BACE-1 assay. Unfortunately, the low compound permeability coupled with unacceptable P-gp efflux liability led to a lack of efficacy in *wild type* animal models that express P-gp at their blood–brain barrier for acute reductions of brain Aβ following oral dosing. Subsequent efforts to address these liabilities will be reported in due course.

Table 5
SAR of appended aromatic rings

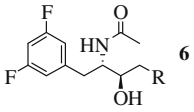

#[a]	R	BACE IC_{50}[b] (nM)	Cat D IC_{50}[c] (nM)	Cell ED_{50}[d] (nM)
56	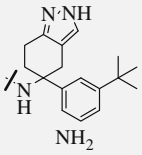	12	300	2.1
57	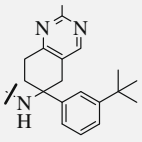	14	210	1.8
58	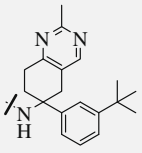	93	910	15

[a] All compounds are 1:1 mixture of epimers.
[b] See Ref. 17.
[c] See Ref. 18.
[d] See Ref. 19.

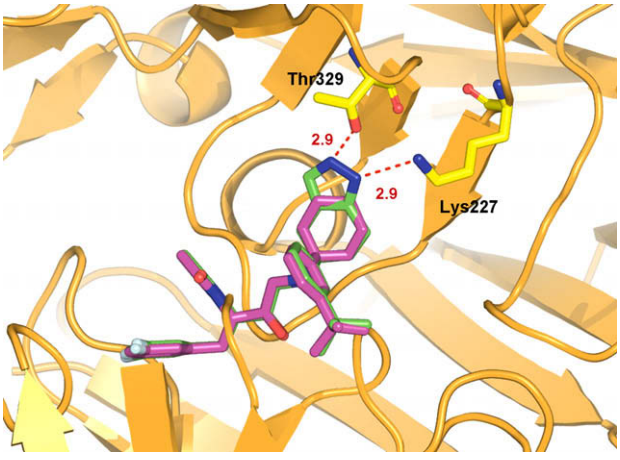

Figure 5. Crystal structure of truncated (56–455) human BACE-1 bound to the more active diastereomer of **56** in green (2.2 Å resolution) overlaid with compound **1** in magenta. The pyrazole is depicted hydrogen bonding to the 'top' residues, Lys227 and Thr329. The PBD deposition code is 3ivi.

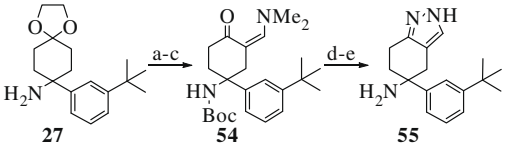

Scheme 5. Reagents and conditions: (a) $(Boc)_2O$, 1,2-DCE, 60 °C, 85%; (b) AcOH, H_2O, 75 °C, 98%; (c) *tert*-butoxybis(dimethylamino)methane, 80 °C; (d) NH_2NH_2–H_2O, glacial AcOH, EtOH, 74% over two steps; (e) 4 N HCl in dioxane 100%.

Table 6
Permeability and P-gp efflux of selected inhibitors

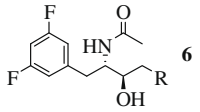

#	R	BACE IC_{50}[a] (nM)	P_{app}[b] (nm/s)	P-gp efflux ratio[c]
1	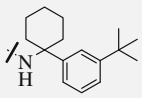	47	7	19
8	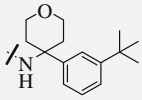	61	81	18
33	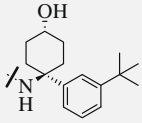	24	3	51
56[d]	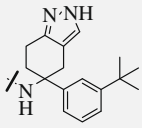	12	16	10

[a] See Ref. 17.
[b] See Ref. 22.
[c] See Ref. 23.
[d] 1:1 mixture of epimers.

Acknowledgements

We would like to thank Ronald Morgan, Wes Zmolek, Jackie Kwong, Lee Latimer, Jill Labbe, Nancy Jewett, Pam Keim, Chris Foster, Christine Olivero, Heather Runes, and Colin Lorentzen for their contributions to this work.

Supplementary data

Supplementary data associated with this article can be found, in the online version, at doi:10.1016/j.bmcl.2009.09.061.

References and notes

1. Ferri, C.; Prince, M.; Brayne, C.; Brodaty, H.; Fratiglioni, L.; Ganguli, M.; Hall, K.; Hasegawa, K.; Hendrie, H.; Huang, Y. *Lancet* **2005**, *366*, 2112.
2. Hardy, J.; Selkoe, D. J. *Science* **2002**, *297*, 353.
3. Sinha, S.; Liberburg, I. *Proc. Natl. Acad. Sci. U.S.A.* **1999**, *96*, 11049.
4. (a) Truong, A. P.; Aubele, D. A.; Probst, G. D.; Neitzel, M. L.; Semko, C. M.; Bowers, S.; Dressen, D.; Hom, R. K.; Konradi, A. W.; Sham, H. L.; Garofalo, A. W.; Keim, P. S.; Wu, J.; Dappen, M. S.; Wong, K.; Goldbach, E.; Quinn, K. P.; Sauer, J.-M.; Brigham, E. F.; Wallace, W.; Nguyen, L.; Hemphill, S. S.; Bova, M. P.; Basi, G. *Bioorg. Med. Chem. Lett.* **2009**, *19*, 4920; (b) Sankaranarayanan, S.; Holahan, M. A.; Colussi, D.; Crouthamel, M.-C.; Devanarayan, V.; Ellis, J.; Espeseth, A.; Gates, A. T.; Graham, S. L.; Gregro, A. R.; Hazuda, D.; Hochman, J. H.; Holloway, K.; Jin, L.; Kahana, J.; Lai, M.-T.; Lineberger, J.; McGaughey, G.; Moore, K. P.; Nantermet, P.; Pietrak, B.; Price, E. A.; Rajapakse, H.; Stauffer, S.; Steinbeiser, M. A.; Seabrook, G.; Selnick, H. G.; Shi, X.-P.; Stanton, M. G.; Swestock, J.; Tugusheva, K.; Tyler, K. X.; Vacca, J. P.; Wong, J.; Wu, G.; Xu, M.; Cook, J. J.; Simon, A. J. *J. Pharmacol. Exp. Ther.* **2009**, *328*, 131; (c) Hussain, I.; Hawkins, J.; Harrison, D.; Hille, C.; Wayne, G.; Cutler, L.; Buck, T.; Walter, D.; Demont, E.; Howes, C.; Naylor, A.; Jeffrey, P.; Gonzalez, M. I.; Dingwell, C.; Michel, M.; Redshaw, S.; Davis, J. B. *J. Neurochem.* **2007**, *100*, 802; (d) Nishitomi, K.; Sakaguchi, G.; Horikoshi, Y.; Gray, A. J.; Maeda, M.; Hirata-Fukae, C.; Becker, A. G.; Hosono, M.; Sakaguchi, I.; Minami, S. S.; Nakajima, Y.; Li, H.-F.; Takeyama, C.; Kihara, T.; Ota, A.; Wong, P. C.; Aisen, P. S.; Kato, A.; Kinoshita, N.; Matsuoka, Y. *J. Neurochem.* **2006**, *96*, 1; (e) Dovey, H. F.; John, V.; Anderson, J. P.; Chen, L. Z.; de Saint Andrieu, P.; Fang, L. Y.; Freedman, S. B.; Folmer, B.; Goldbach, E.; Holsztynska, E. J.; Hu, K. L.; Johnson-Wood, K. L.; Kennedy, S. L.; Kholodenko, D.; Knops, J. E.; Latimer, L. H.; Lee, M.; Liao, Z.; Lieberburg, I. M.; Motter, R. N.; Mutter, L. C.; Nietz, J.; Quinn, K. P.; Sacchi, K. L.; Seubert, P. A.; Shopp, G. M.; Thorsett, E. D.; Tung, J. S.; Wu, J.; Yang, S.; Yin, C. T.; Schenk, D. B.; May, P. C.; Altstiel, L. D.; bender, M. H.; Boggs, L. N.; Britton, T. C.; Clemens, J. C.; Czilli, D. L.; Dieckman-McGinty, D. K.; Droste, J. J.; Fuson, K. S.; Gitter, B. D.; Hyslop, P. A.; Johnstone, E. M.; Li, W.-Y.; Little, S. P.; Mabry, T. E.; Miller, F. D.; Ni, B.; Nissen, J. S.; Porter, W. J.; Potts, B. D.; Reel, J. K.; Stephenson, D.; Su, Y.; Shipley, L. A.; Whitesitt, C. A.; Yin, T.; Audia, J. E. *J. Neurochem.* **2001**, *76*, 173.
5. Schmidt, B.; Baumann, S.; Braun, H. A.; Larbig, G. *Curr. Top. Med. Chem.* **2006**, *6*, 377.
6. Lleo, A. *Curr. Top. Med. Chem.* **2008**, *8*, 9.
7. (a) Wong, G. T.; Manfras, D.; Poulet, F. M.; Zhang, Q.; Josien, H.; Bara, T.; Engstrom, L.; Pinzon-Ortiz, M.; Fine, J. S.; Lee, H.-J. J.; Zhang, L.; Higgins, G. A.; Parker, E. M. *J. Biol. Chem.* **2004**, *279*, 12876; (b) Milano, J.; McKay, J.; Dagenais, C.; Foster-Brown, L.; Pognan, F.; Gadient, R.; Jacobs, R. T.; Zacco, A.; Greenberg, B.; Ciaccio, P. J. *Toxicol. Sci.* **2004**, *82*, 341; (c) Searfoss, G. H.; Jordan, W. H.; Calligaro, D. O.; Galbreath, E. J.; Schirtzinger, L. M.; Berridge, B. R.; Gao, H.; Higgins, M. A.; May, P. C.; Ryan, T. P. *J. Biol. Chem.* **2003**, *278*, 46107; (d) Doerfler, P.; Shearman, M. S.; Perlmutter, R. M. *Proc. Natl. Acad. Sci. U.S.A.* **2001**, *98*, 9312; (e) Hadland, B. K.; Manley, N. R.; Su, D.-M.; Longmore, G. D.; Moore, C. L.; Wolfe, M. S.; Schroeter, E. H.; Kopan, R. *Proc. Natl. Acad. Sci. U.S.A.* **2001**, *98*, 7487.
8. (a) Luo, Y.; Bolon, B.; Kahn, S.; Bennett, B. D.; Babu-Khan, S.; Denis, P.; Fan, W.; Kha, H.; Zhang, J.; Gong, Y.; Martin, L.; Louis, J.-C.; Yan, Q.; Richards, W.; Citron, M.; Vassar, R. *Nat. Neurosci.* **2001**, *4*, 231; (b) Cai, H.; Wang, Y.; McCarthy, D.; Wen, H.; Borchelt, D. R.; Price, D. L.; Wong, P. C. *Nat. Neurosci.* **2001**, *4*, 233; (c) Roberds, S. L.; Anderson, J.; Basi, G.; Bienkowski, M.; Branstetter, D. G.; Chen, K. S.; Freedman, S. B.; Frigon, N. L.; Games, D.; Hu, K.; Johnson-Wood, K.; Kappenman, K. E.; Kawabe, T. T.; Kola, I.; Keuhn, R.; Lee, M.; Liu, W.; Motter, R.; Nichols, N. F.; Power, M.; Robertson, D. W.; Schenk, D.; Schoor, M.; Shopp, G. M.; Shuck, M. E.; Sinha, S.; Svensson, K. A.; Tatsuno, G.; Tintrup, H.; Wijsman, J.; Wright, S.; McConlogue, L. *Hum. Mol. Genet.* **2001**, *10*, 1317.
9. Luo, Y.; Bolon, B.; Damore, M. A.; Fitzpatrick, D.; Liu, H.; Zhang, J.; Yan, Q.; Vassar, R.; Citron, M. *Neurobiol. Dis.* **2003**, *14*, 81.
10. McConlogue, L.; Buttini, M.; Anderson, J. P.; Brigham, E. F.; Chen, K. S.; Freedman, S. B.; Games, D.; Johnson-Wood, K.; Lee, M.; Zeller, M.; Liu, W.; Motter, R.; Sinha, S. *J. Biol. Chem.* **2007**, *282*, 26326.
11. Nikolaev, A.; McLaughlin, T.; O'Leary, D. D. M.; Teesier-Lavign, M. *Nature* **2009**, *457*, 981.
12. (a) Steinfeld, R.; Reinhardt, K.; Schreiber, K.; Hillebrand, M.; Kraetzner, R.; Brück, W.; Saftig, P.; Gärtner, J. *Am. J. Hum. Genet.* **2006**, *78*, 988; (b) Sintola, E.; Partanen, S.; Strömme, P.; Haapanen, A.; Haltia, M.; Maehlen, J.; Lehesjoki, A.-E.; Tyynelä, J. *Brain* **2006**, *129*, 1438; (c) Koikie, M.; Nakanishi, H.; Saftig, P.; Ezaki, J.; Isahara, K.; Ohsawa, Y.; Schulz-Schaeffer, W.; Watanabe, T.; Waguri, S.; Kametaka, S.; Shibata, M.; Yamamoto, K.; Kominami, E.; Peters, C.; von Figura, K.; Uchiyama, Y. *J. Neurosci.* **2000**, *20*, 6898.
13. Brady, S. F.; Singh, S.; Crouthamel, M.-C.; Holloway, M. K.; Cobrurn, C. A.; Garsky, V. M.; Bogusky, M.; Pennington, M. W.; Vacca, J. P.; Hazuda, D.; Lai, M.-T. *Bioorg. Med. Chem. Lett.* **2004**, *14*, 601.
14. John, V.; Hom, R.; Sealy, J.; Aquino, J.; Probst, G.; Tung, J.; Fang, L. WO2005070407, 2005.
15. Toth, G.; Bowers, S. G.; Truong, A. P.; Probst, G. *Curr. Pharm. Des.* **2007**, *13*, 3476.
16. Reeder, M. R. WO2002085877, 2002.
17. Compounds serially diluted in DMSO were added to recombinant BACE purified from *E. coli* in 100 mM sodium acetate buffer containing 0.001% Tween-20 at pH 4.5 and allowed to incubate for 20 min at room temperature. A biotinylated peptide substrate, based on the Swedish mutant APP sequence, containing an Oregon Green moiety at the C-terminus, was added to initiate the reaction which was allowed to proceed for 3 h at 37 °C. The reaction was quenched by the addition of a fivefold volume excess of 100 mM sodium phosphate buffer pH 7.4 containing a 1.5 μM final concentration of streptavidin. The extent of fluorescence polarization was measured using a LJL Analyst.
18. The cathepsin-D was obtained from Sigma (cat. #C8696). Cathepsin-D was first dissolved with water to a 2 μM concentration and then subsequently with 100 mM sodium acetate buffer pH 4.5 to a 1.8 nM working concentration. A biotinylated peptide cathepsin-D substrate was labeled at the C-terminus of the peptide with an Oregon Green fluorophore. Compounds were serially diluted threefold in DMSO at a 100× concentration and then subsequently diluted 33× with 100 mM sodium acetate buffer pH 4.5. Compound was added to cathepsin-D (0.6 nM final concentration) for 30 min before the addition of peptide substrate to initiate the reaction. The reaction was allowed to proceed for 110 min at 37 °C and then quenched by the addition of streptavidin in 200 mM sodium phosphate buffer pH 7.5. The amount of fluorescence polarization in the well was measured using a LJL Analyst (Perkin Elmer). If cathepsin-D cleaves the peptide substrate then polarization will be reduced.
19. (a) Ref. 4e in which the HEK 293 cells were modified to express the Swedish mutation of APP FAD isoform.; (b) Johnson-Wood, K.; Lee, M.; Motter, R.; Hu, K.; Gordon, G.; Barbour, R.; Khan, K.; Gordon, M.; Tan, H.; Games, D.; Lieberburg, I.; Schenk, D.; Seubert, P.; McConlogue, L. *Proc. Natl. Acad. Sci. U.S.A.* **1997**, *94*, 1550; (c) Seubert, P.; Vigo-Pelfrey, C.; Esch, F.; Lee, M.; Dovey, H.; Davis, D.; Sinha, S.; Schlossmacher, M.; Whaley, J.; Swindlehurst, C.; McCormack, R.; Wolfert, R.; Selkoe, D.; Lieberburg, I.; Schenk, D. *Nature* **1992**, *359*, 325.
20. Beare, N. A.; Hartwig, J. F. *J. Org. Chem.* **2002**, *67*, 541.
21. Kalgutkar, A. S.; Obach, S. R.; Maurer, T. S. *Curr. Drug Metab.* **2007**, *8*, 407.
22. Compounds (5 μM) in mHBSS (pH 7.4) were incubated with MDCK II cell monolayers for 120 min at 37 °C. Samples were taken from apical and basolateral chambers, and analyzed using LC/MS/MS.
23. Compounds (5 μM) in mHBSS (pH 7.4) were incubated with MDR1-MDCK cell monolayers for 120 min at 37 °C with and without a P-gp inhibitor. Samples were taken from apical (A) and basolateral (B) chambers, and analyzed using LC/MS/MS. The efflux ratio was determined by dividing the rate of the A to B direction with and without a P-gp inhibitor.
24. Falgueyret, J. P.; Desmarais, S.; Oballa, R.; Black, C. W.; Cromlish, W.; Khougaz, K.; Lamonyagne, S.; Masse, F.; Riendeau, D.; Toulmond, S.; Percival, D. M. *J. Med. Chem.* **2005**, *48*, 7535.